DINAME 2023 - Proceedings of the XIX International Symposium on Dynamic Problems of Mechanics,
A.S. De Paula, A.T. Fabro and M.R. Machado (Editors), ABCM.
Pirenópolis, Go, Brazil, February 26th to March 3rd, 2023

Identification of damping with a high-speed camera

Ivan Tomac[1,2], **Janko Slavič**[1]

[1] University of Ljubljana, Faculty of Mechanical Engineering, Aškerčeva cesta 6, SI-1000 Ljubljana, Slovenia

[2] University of Split, Faculty of Electrical Engineering, Mechanical Engineering and Naval Architecture, Ruđera Boškovića 32, HR-21000 Split, Croatia

Abstract: The use of high-speed cameras in the field of structural dynamics for modal identification is a challenging task. High-speed cameras offer several advantages over classical measurement techniques, such as non-contact full-field measurement from a distance. However, it is not easy to obtain as good a measurement as with classical techniques, since various influences play a role, such as: light source, excitation strength, strong noise and the measured displacement, which becomes very small at high frequencies. This makes modal identification from such data very difficult with classical methods, especially when it comes to identifying structural damping. Identifying damping is a challenging task, even with high dynamic range sensors (accelerometers).The main advantage of high-speed camera measurement is the availability of a full-field response, which can be used as an advantage to reduce the uncertainty of the identified results. Due to the high noise, an advanced signal processing method must be used that is able to localise a good portion of the signal and identify damping. Such a method is based on the continuous wavelet transform, which provides very good frequency separation. It is resistant to noise and much faster than the continuous wavelet transform. It is a Morlet-Wave Damping identification method which can be understood as a microscope for the signal we used in this study to identify damping. Damping is a modal parameter that is theoretically not spatially dependent. Therefore, we used spatial overdetermination to increase the accuracy of the damping identification. The full-filed damping identification results were averaged over the identified deflection shapes. The method was tested experimentally on the simple structure up to 2.5 kHz. The results were found to be comparably accurate to the damping identified using the piezoelectric accelerometer with high-dynamic-range and low-noise piezoelectric accelerometer, proving that damping can be accurately identified using high-speed camera measurements, only.

Keywords: Morlet-wave, damping, spatial distribution, full-field

INTRODUCTION

High-speed cameras are increasingly used in the field of structural dynamics Helfrick et al. (2011); Siebert et al. (2009), where they allow non- contact measurements of displacements with a high spatial resolution. Theoretically, each pixel can be a sensor enabling full-field measurement Beberniss and Ehrhardt (2017); Durand-Texte et al. (2020). One of the advantages is that high-speed camera measurements provide a full-field response from a remote object Baqersad et al. (2017). Non-contact and remote monitoring enables applications that are not feasible or difficult using conventional approaches.

This paper is an abridged version of the research published in Tomac and Slavič (2022a). The focus of this research is to overcome the relatively noisy measurements obtained with high-speed cameras by taking advantage of the overdetermination that this full-field measurement offers. At the same time, the uncertainty in the damping- identification is spatially dependent (higher at the nodes). Damping identification is based on the Morlet-Wave Damping Identification (MWDI) method Slavič and Boltežar (2011), which was previously shown to have the advantages of the Continuous Wavelet Transform method (CWT), e.g. identification on short signals, resistance to noise, good frequency separation, Slavič et al. (2003); Staszewski (1997); however, MWDI is numerically much less demanding Slavič and Boltežar (2011); Tomac et al. (2017).

THEORETICAL BACKGROUND

This section describes the theoretical basis for identifying damping using the Morlet-Wave Damping Identification (MWDI) method Slavič and Boltežar (2011) and the Extended MWDI method Tomac et al. (2017).

MWDI method

The MWDI method is based on the continuous wavelet transform and the damping is identified from the ratio of only two wavelet coefficients calculated as the inner product between the signal $f_\mathrm{m}(t)$ and the basic wavelet function $\psi(t)$ using the following expression:

$$I_{1,2}(n,k,\omega) = \int_0^T f_\mathrm{m}(t)\,\psi^*(n_{1,2},k,\omega,t)\,\mathrm{d}t, \tag{1}$$

where T is the time length of the analysed mode, defined for reasons of spectral-leakage by the number of oscillations k ($k \in \mathbb{N}$) at the analysed frequency ω: $T = 2\pi k/\omega$; * is the complex conjugate and ψ is a Morlet wavelet function.

To identify the damping, one must obtain two MW integrals with different time spread parameters n_1 and n_2, where $n_1 < n_2$ Slavič and Boltežar (2011). The MW integrals are shown graphically in Fig. 1 in contrast to the numerically simulated response. One obtains the ratio between MW integrals:

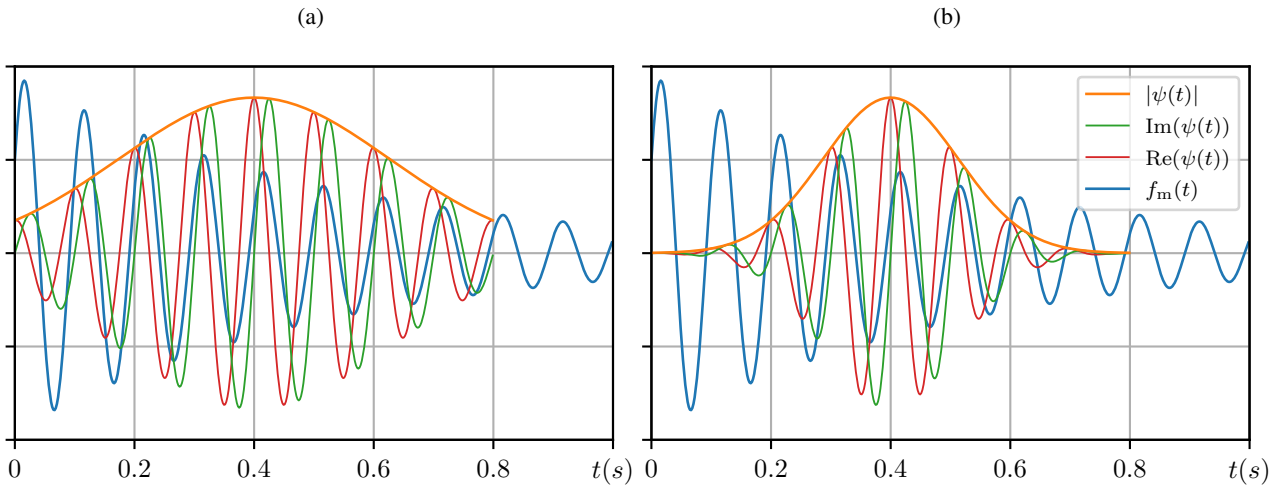

Figure 1: Free response and MW function with $k = 8$, $\omega = 10 \cdot 2\pi$ Hz and a) $n_1 = 5$, b) $n_2 = 10$.

$$\tilde{M}\left(n_1, n_2, k, \omega\right) = \frac{|I(n_1, k, \omega)|}{|I(n_2, k, \omega)|} \tag{2}$$

The same ratio is expressed analytically – $M\left(n_1, n_2, k, \delta\right)$ Slavič and Boltežar (2011), which allows to establish the following equation:

$$\tilde{M}\left(n_1, n_2, k_i, \omega_i\right) - M\left(n_1, n_2, k_i, \delta_i\right) = 0 \tag{3}$$

which is solved for the unknown damping ratio δ_i of the i-th mode. The method is implemented as a Python package mwdi Tomac and Slavič (2022c).

eMWDI method

Tomac et al. (2017) discovered that the MWDI method is sensitive to the selection of MW function parameters. To overcome the parameter selection problem, the optimisation approach is introduced as an extension of the MWDI method to achieve a convergent result. The method was originally developed for identifying the damping from a single measurement point in the full range of possible parameters k and n_2, with the parameter n_1 held constant. For details see Tomac and Slavič (2022a); Tomac et al. (2017).

In this study, the extended MWDI was used in the search for the parameter $k \in \mathbb{N}$ between a small set of spatial points for the fixed parameter n_2, which is typically chosen to be twice as high as the parameter value n_1 Slavič and Boltežar (2011). The spatial PSD is used to select locations suitable for the optimisation approach to select the parameter k_i for each mode i. The damping is identified in a predefined range of k parameters for the selected locations, where the optimal k is selected by finding the minimum standard deviation of the damping $\delta_{i,l}(k)$ between selected spatial locations l:

$$k_i = \arg\min_k \left\{ \operatorname*{std\,dev}_l \left\{ \delta_{i,l}\left(k\right) \right\} \right\} \tag{4}$$

The method is implemented in the Python package extended-mwdi Tomac and Slavič (2022b).

SPATIALLY WEIGHTED MWDI BASED ON THE EXPERIMENTAL DATA

The identification procedure is shown in the diagram in Fig. 2, where the user's input is shown with red arrows and the green arrows with the results of the individual steps. The procedure includes six steps based on the experimental results used in Tomac and Slavič (2022a).

Step #1: Identification of displacements

The identification is carried out on the laboratory example of the aluminium beam ($w \times h \times d = 600 \times 12 \times 50$ mm) which was freely supported on two polyurethane foam blocks. Excitation was done with a modal hammer and the response was measured simultaneously with a high-speed camera (Photron FASTCAM SA -Z type 2100K-M-64GB) and

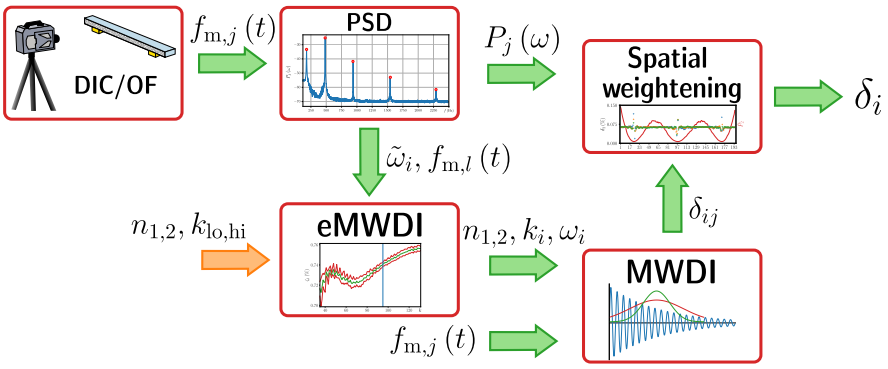

Figure 2: Procedure for identifying damping. The indices are: i for modes, j for spatial location and l for selected spatial locations.

accelerometer (DYTRAN 3097A2T). The locations of the excitation and the response, including the speckle type, can be seen in Fig. 3. The displacement is identified using the Lucas-Kanade method Lucas and Kanade (1981), as implemented

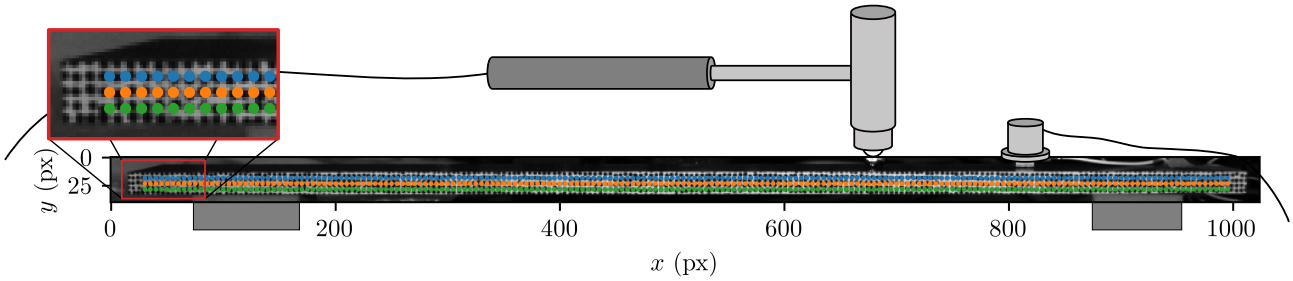

Figure 3: A single image from the high-speed camera view showing the speckle type and the points identifying the displacement (the colours correspond to: blue – top, orange – middle and green – bottom row).

in the open-source pyIDI Zaletelj et al. (2020) package, at locations 194 $times 3 = 582$, shown with dots in Fig. 3. The time response identified from the upper left point is shown in Fig 4.

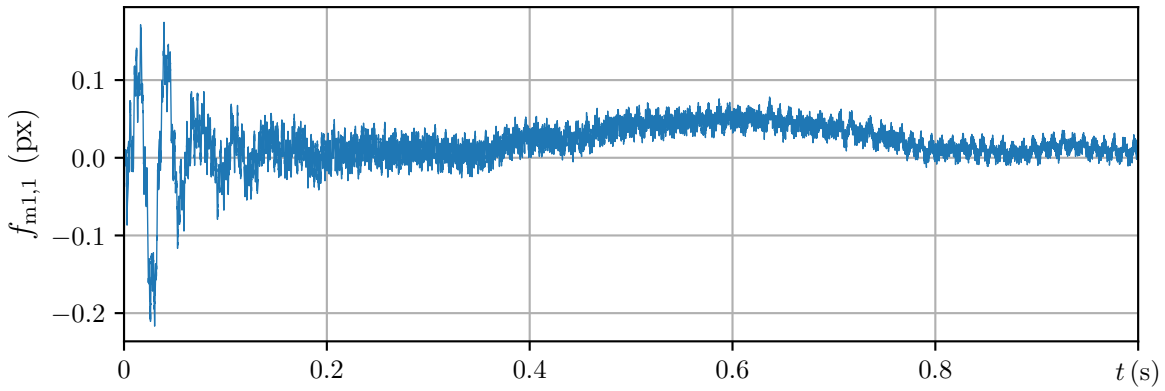

Figure 4: High-speed camera-based displacement at a point on the upper left.

Step #2: Rough estimation of natural frequencies for PSD

The MWDI method assumes that the frequencies of the modes are known. One obtains the power spectral density from the full field time measurements:

$$P_j(\omega) = \frac{1}{T}\,\hat{f}^*_{\mathrm{m},j}(\omega)\,\hat{f}_{\mathrm{m},j}(\omega) \tag{5}$$

The PSDs obtained are summed to eliminate the noise and the natural frequencies are selected from the diagram shown in Fig. 5 which contains their values.

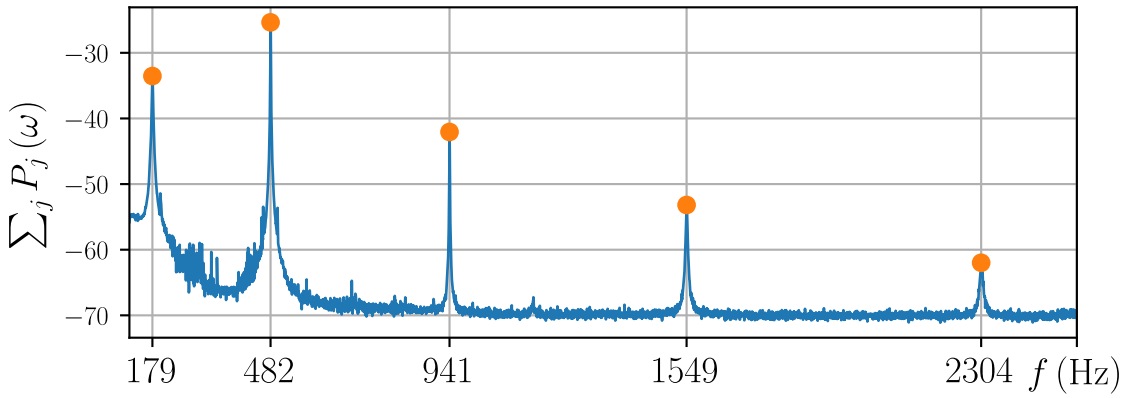

Figure 5: High-speed camera-based displacement at a point on the upper left.

Step #3: Spatial Power Spectral Density

The spatial PSDs are used for two purposes, which can be seen in Fig. 2. The first purpose is to perform spatial averaging in the later step of the full-fiel damping results and the second purpose is to select the points to be used with the extended MWDI to select the optimal k_i parameters for each mode. The spatial PSD is obtained by applying a narrow rectangular window $\Delta f = \pm 5$ Hz around each natural frequency for all locations as shown in Fig. 6 using the second mode as an example.

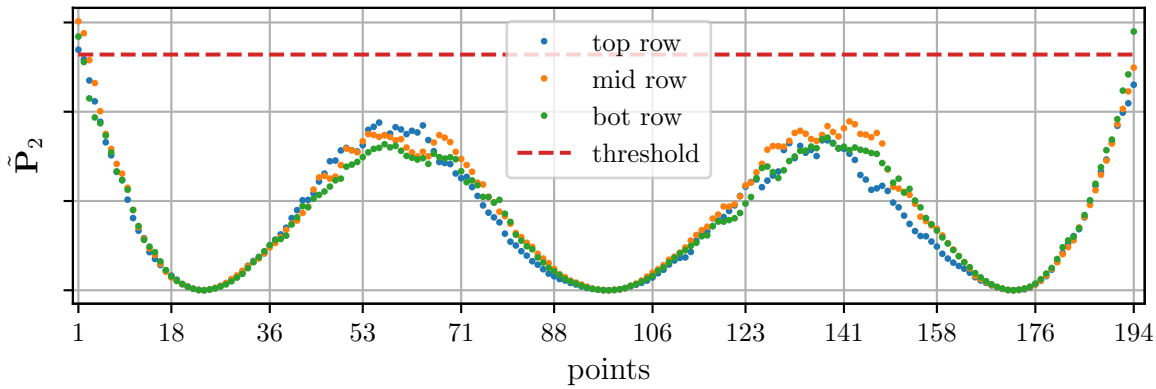

Figure 6: Spatial distribution of the energy spectra for the second mode with threshold used for extended MWDI.

Step #4: extended MWDI – find optimal k

The procedure for finding the optimal k parameter uses the roughly estimated natural frequencies. The search is performed at the top (1 %) points, which are selected separately for each mode using the spatial PSD from the previous step. The selected points can be seen in the example of the second mode in Fig. 6, separated by a dashed red line. The range of k parameters is set between $30 \leq k \leq 600$ and the time spread parameters are set to high sensitivity Tomac and Slavič (2022a) as $n_1 = 5$ and $n_2 = 10$. The optimal parameter k is selected using the Eq. (4) and the result of the optimisation is shown in Fig. 7 using the second mode as an example. During the optimisation process, the exact natural frequency is also identified. It is identified by finding the maximum of the MW integral (1):

$$\frac{\partial}{\partial \omega} |I(n, k_i, \omega)| = 0 \tag{6}$$

numerically in the narrow frequency band around the roughly estimated natural frequency. The optimal k values and the exact natural frequencies for the individual modes are listed in Tab. 1.

Step #5: MWDI – Full-field damping identification

Using the optimal k values and the exact natural frequencies from the previous step in Tab. 1, the full-filed damping identification is performed. This step executes very quickly, in a few seconds, due to the efficiency of the MWDI method, unlike the previous step. The results of the full filed damping identification are shown in Fig. 8 using the example of the third mode with the corresponding spatial PSD. Based on the full-field results, it can be observed how the uncertainty of the identified results increases as expected with increasing proximity to the nodes.

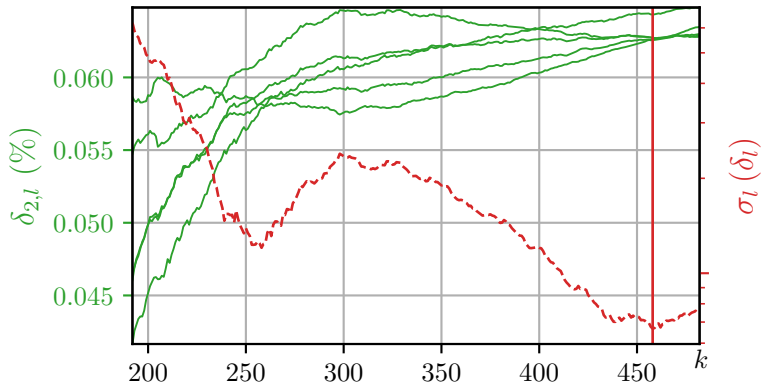

Figure 7: Example of an optimisation procedure for selecting the optimal k value using the example of the second mode.

Table 1: Optimal k values obtained with extended MWDI method.

Mode:	1st	2nd	3rd	4th	5th
Optimal: k	95	458	570	342	554
Exact: f_n (Hz)	179.21	482.22	941.15	1549.1	2304.7

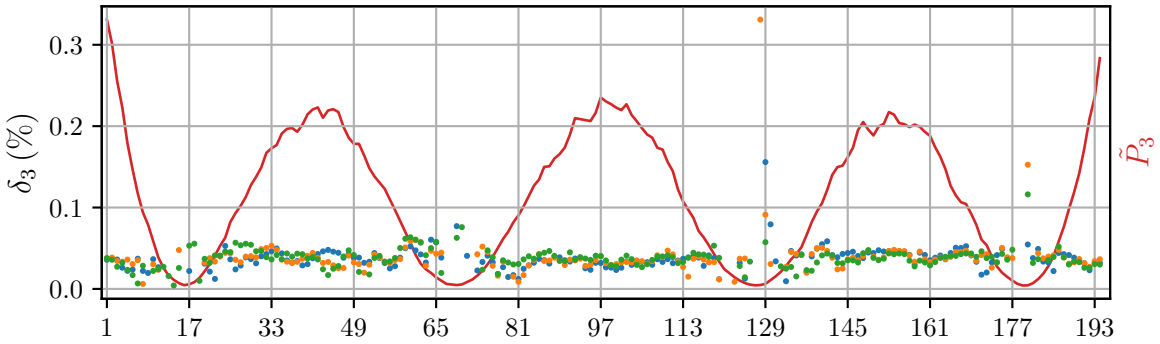

Figure 8: Full-field damping identified with the MWDI method for the third mode, the red solid line is the corresponding spatial PSD.

Step #6: Spatial weighting

The full-field damping ratios are spatially weighted to obtain the modal damping ratio δ_i. The spatial PSD is a good choice for weighting to exclude results near nodes. A single damping value is obtained using the following expression:

$$\delta = \frac{1}{\sum_j P_j} \sum_j P_j \, \delta_j \tag{7}$$

for each mode and the results are shown in Tab. 2.

Verification of the results based on the high-speed camera is done by comparing the results with the data measured exclusively with the accelerometer. The damping is identified using the MWDI method, using the same input values as in step #4 for the full-field identification of the damping. The results are shown in tab 2, including the comparison with the accelerometer expressed as a relative error calculated with: $\text{error}_i = (\delta_i - \delta_{\text{acc},i}) / \delta_{\text{acc},i} \cdot 100\ \%$.

Table 2: Identification results from HS camera and accelerometer data.

Natural frequency:	1st	2nd	3rd	4th	5th
δ (%)	0.7508	0.0633	0.0358	0.1041	0.1482
δ_{acc} (%)	0.7443	0.0633	0.0364	0.1054	0.1567
error (%)	0.87	-0.06	-1.64	-1.21	-5.43

CONCLUSIONS

The methodology for identifying structural damping from responses obtained from high-speed video recording was presented using data from a laboratory test as an example. The experimental results of this research confirmed that the high-speed camera-based approach to damping identification can lead to similar accuracy of damping identification as identification based on high dynamic range sensors.

This confirms the high-precision, non-contact identification of damping based on camera measurements, which opens up new possibilities for structural health monitoring and failure analysis.

ACKNOWLEDGMENTS

The authors gratefully acknowledge partial financial support from the European Union's Horizon 2020 research and innovation programme under Marie Skłodowska-Curie Grant Agreement No. 101027829 and the Slovenian Research Agency (N2-0144).

REFERENCES

J. Baqersad, P. Poozesh, C. Niezrecki, and P. Avitabile. Photogrammetry and optical methods in structural dynamics – a review. *Mechanical Systems and Signal Processing*, 86:17–34, 2017. ISSN 0888-3270. doi: 10.1016/j.ymssp.2016.02.011. URL https://doi.org/10.1016/j.ymssp.2016.02.011.

T. J. Beberniss and D. A. Ehrhardt. High-speed 3d digital image correlation vibration measurement: Recent advancements and noted limitations. *Mechanical Systems and Signal Processing*, 86:35–48, 2017. ISSN 0888-3270. doi: 10.1016/j.ymssp.2016.04.014.

T. Durand-Texte, M. Melon, E. Simonetto, S. Durand, and M.-H. Moulet. Single-camera single-axis vision method applied to measure vibrations. *Journal of Sound and Vibration*, 465:115012, 2020. ISSN 0022-460X. doi: 10.1016/j.jsv.2019.115012.

M. N. Helfrick, C. Niezrecki, P. Avitabile, and T. Schmidt. 3d digital image correlation methods for full-field vibration measurement. *Mechanical Systems and Signal Processing*, 25:917–927, 2011. ISSN 0888-3270. doi: 10.1016/j.ymssp.2010.08.013.

B. D. Lucas and T. Kanade. An iterative image registration technique with an application to stereo vision. pages 674–679. Morgan Kaufmann Publishers Inc., 1981. URL https://dl.acm.org/doi/10.5555/1623264.1623280.

T. Siebert, R. Wood, and K. Splitthof. High speed image correlation for vibration analysis. *Journal of Physics: Conference Series*, 181:12064, 8 2009. doi: 10.1088/1742-6596/181/1/012064.

J. Slavič and M. Boltežar. Damping identification with the morlet-wave. *Mechanical Systems and Signal Processing*, 25:1632–1645, 7 2011. ISSN 08883270. doi: 10.1016/j.ymssp.2011.01.008. URL https://doi.org/10.1016/j.ymssp.2011.01.008.

J. Slavič, I. Simonovski, and M. Boltežar. Damping identification using a continuous wavelet transform, application to real data. *Journal of Sound and Vibration*, 262:291–307, 2003. doi: 10.1016/S0022-460X(02)01032-5.

W. J. Staszewski. Identification of damping in mdof systems using time-scale decomposition. *Journal of sound and vibration*, 203:283–305, 1997. doi: 10.1006/jsvi.1996.0864.

I. Tomac and J. Slavič. Damping identification based on a high-speed camera. *Mechanical Systems and Signal Processing*, 166:108485, 3 2022a. ISSN 08883270. doi: 10.1016/j.ymssp.2021.108485. URL https://linkinghub.elsevier.com/retrieve/pii/S0888327021008281.

I. Tomac and J. Slavič. itomac/extended morlet-wave: emwdi v0.3.1, 8 2022b. URL https://doi.org/10.5281/zenodo.6979893.

I. Tomac and J. Slavič. ladisk/mwdi: Mwdi v0.71, 8 2022c. URL https://doi.org/10.5281/zenodo.7002813.

I. Tomac, Ž. Lozina, and D. Sedlar. Extended morlet-wave damping identification method. *International Journal of Mechanical Sciences*, 127, 2017. ISSN 00207403. doi: 10.1016/j.ijmecsci.2017.01.013. URL https://doi.org/10.1016/j.ijmecsci.2017.01.013.

K. Zaletelj, D. Gorjup, and J. Slavič. ladisk/pyidi: Release of the version v0.23, 9 2020. URL https://doi.org/10.5281/zenodo.4017153.

RESPONSIBILITY NOTICE

The author(s) is (are) the only responsible for the printed material included in this paper.